Optofluidic notch filter integration by lift-off of thin films

Brian S. Phillips[1], Philip Measor[2], Yue Zhao[1], Holger Schmidt[2], and Aaron R. Hawkins[1*]

[1]ECEn Department, Brigham Young University, 459 Clyde Building, Provo, UT 84602, USA
[2]School of Engineering, University of California Santa Cruz, 1156 High Street, Santa Cruz, CA 95604, USA
[*]hawkins@ee.byu.edu

Abstract: Optofluidic platforms used for biomolecular detection require spectral filtering for distinguishing analyte signals from unwanted background. Towards a fully integrated platform, an on-chip filter is required. Selective deposition of dielectric thin films on an optofluidic sensor based on antiresonant reflecting optical waveguide (ARROW) technology provides the means for localized, on-chip optical filtering. We present a lift-off technique, compatible with thin-film processing including plasma-enhanced chemical vapor and sputtering deposition. The resulting optofluidic notch filters exhibited a 20 dB rejection with linewidths as low as 20 nm for ~1 cm long chips consisting of liquid-core and solid-core waveguides.

OCIS codes: (130.7408) Wavelength Filter Devices; (130.0130) Integrated Optics.

References and links

1. D. Psaltis, S. R. Quake, and C. Yang, "Developing optofluidic technology through the fusion of microfluidics and optics," Nature **442**(7101), 381–386 (2006).
2. C. L. Bliss, J. N. McMullin, and C. J. Backhouse, "Integrated wavelength-selective optical waveguides for microfluidic-based laser-induced fluorescence detection," Lab Chip **8**(1), 143–151 (2007).
3. A. H. J. Yang, S. D. Moore, B. S. Schmidt, M. Klug, M. Lipson, and D. Erickson, "Optical manipulation of nanoparticles and biomolecules in sub-wavelength slot waveguides," Nature **457**(7225), 71–75 (2009).
4. M. A. Duguay, Y. Kokubun, T. L. Koch, and L. Pfeiffer, "Antiresonant reflecting optical waveguides in SiO_2-Si multilayer structures," Appl. Phys. Lett. **49**(1), 13–15 (1986).
5. H. Schmidt, and A. R. Hawkins, "Optofluidic waveguides: I. Concepts and implementations," Microfluid. Nanofluid. **4**(1-2), 3–16 (2008).
6. P. Measor, L. Seballos, D. Yin, J. Z. Zhang, E. J. Lunt, A. R. Hawkins, and H. Schmidt, "On-chip surface-enhanced Raman scattering detection using integrated liquid-core waveguides," Appl. Phys. Lett. **90**(21), 211107 (2007).
7. D. Yin, E. J. Lunt, M. I. Rudenko, D. W. Deamer, A. R. Hawkins, and H. Schmidt, "Planar optofluidic chip for single particle detection, manipulation, and analysis," Lab Chip **7**(9), 1171–1175 (2007).
8. S. Kühn, P. Measor, E. J. Lunt, B. S. Phillips, D. W. Deamer, A. R. Hawkins, and H. Schmidt, "Loss-based optical trap for on-chip particle analysis," Lab Chip **9**(15), 2212–2216 (2009).
9. M. I. Rudenko, S. Kühn, E. J. Lunt, D. W. Deamer, A. R. Hawkins, and H. Schmidt, "Ultrasensitive Qbeta phage analysis using fluorescence correlation spectroscopy on an optofluidic chip," Biosens. Bioelectron. **24**(11), 3258–3263 (2009).
10. A. R. Hawkins, and H. Schmidt, "Optofluidic waveguides: II. Fabrication and structures," Microfluid. Nanofluid. **4**(1-2), 17–32 (2008).
11. D. Yin, D. W. Deamer, H. Schmidt, J. P. Barber, and A. R. Hawkins, "Single-molecule detection sensitivity using planar integrated optics on a chip," Opt. Lett. **31**(14), 2136–2138 (2006).
12. H. Schmidt, D. Yin, J. P. Barber, and A. R. Hawkins, "Hollow-core waveguides and 2D waveguide arrays for integrated optics of gases and liquids," IEEE J. Sel. Top. Quant. **11**(2), 519–527 (2005).
13. J. K. Ranka, R. S. Windeler, and A. J. Stentz, "Visible continuum generation in air-silica microstructure optical fibers with anomalous dispersion at 800 nm," Opt. Lett. **25**(1), 25–27 (2000).
14. P. Yeh, *Optical waves in layered media* (Wiley-Interscience, 1988).
15. K. P. Lor, Q. Liu, and K. S. Chiang, "UV-written long-period gratings on polymer waveguides," IEEE Photon. Technol. Lett. **17**(3), 594–596 (2005).
16. A. Perentos, G. Kostovski, and A. Mitchell, "Polymer long-period raised rib waveguide gratings using nano-imprint lithography," IEEE Photon. Technol. Lett. **17**(12), 2595–2597 (2005).

#121398 - $15.00 USD Received 14 Dec 2009; revised 25 Jan 2010; accepted 29 Jan 2010; published 23 Feb 2010

17. E. J. Lunt, P. Measor, B. S. Phillips, S. Kühn, H. Schmidt, and A. R. Hawkins, "Improving solid to hollow core transmission for integrated ARROW waveguides," Opt. Express **16**(25), 20981–20986 (2008).

1. Introduction

Optofluidics, devices employing both microfluidic channels and integrated optics [1], have recently seen increased utility in experiments such as biomolecular analysis and manipulation in lab-on-a-chip settings [2,3]. Optofluidics based on solid-core and liquid-core antiresonant reflecting optical waveguides (ARROWs) confine light in low-index liquid cores using one or more high-index dielectric cladding layers that effectively act as Fabry-Perot etalons operating on antiresonance, i.e. maximum reflectivity [4,5]. They have been applied in fluorescence detection using a variety of bioparticles and surface enhanced Raman spectroscopy with silver nanoparticles and fluorescent dyes [6–9]. These devices require high discrimination between analyte signals and background noise (e.g. scattered excitation light) for sensitive detection. As these platforms become more highly integrated and require more sensitive detection capabilities, it is natural to move optical filtering on-chip.

ARROW platforms are fabricated using a sacrificial core process and other planar fabrication methods described previously [10]. Wavelength filtering has previously been accomplished by discrete off-chip optical filtering [11]. However, the intrinsic wavelength dependence of the underlying interference effect provides additional design opportunities in ARROWs for integrating spectral filtering on the optofluidic chip itself. It was proposed that by careful thickness design, a waveguide can discriminately confine analyte signal wavelengths while rejecting the excitation light [9,12].

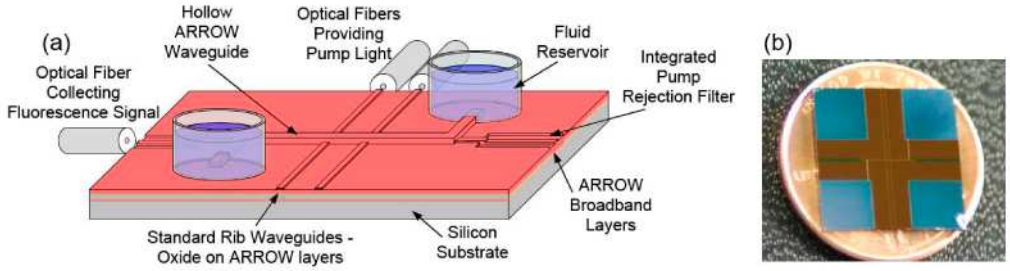

Fig. 1. – ARROW platform with integrated pump rejection filter a) schematic representation, b) fabricated device

The ARROW platform has solid-core waveguides that couple light into and out of the liquid core (Fig. 1). By modifying only the collection waveguides we can efficiently integrate a notch filter to reject any scattered excitation light and pass the red-shifted signal. While visible wavelength filtering is possible with other techniques (e.g. Bragg gratings, interference filters), they often require many dielectric layers (each with low tolerances) or costly emerging nanofabrication processing. In this work, we present a straightforward, fast, and low cost method of patterning different filter and broadband waveguide regions involving a lift-off process and we experimentally demonstrate the completed device. We show that this lift-off technique is compatible with existing ARROW optofluidic platform production methods and demonstrate a notch filter device for efficient narrow-band pump rejection at the HeNe laser wavelength (632.8 nm).

The thin-film layer designs used in the ARROW platform are detailed in Tables 1-3. Table 1 contains a "filter layer" stack deposited over the entire wafer. In order to confine light (λ_{ex}=632.8nm) in a low-index core (SiO_2), on a high-index substrate (Si), the cladding layers (SiN and SiO_2) are made to satisfy the antiresonant condition (e.g. 1st order thickness) [4]. To filter out a specific wavelength (λ_{ex}) and pass a range relevant for Alexa 647 (λ_{em}), a resonant layer (e.g. 4th order thickness) can be deposited within the stack to effectively create high optical loss at the design wavelength.

#121398 - $15.00 USD Received 14 Dec 2009; revised 25 Jan 2010; accepted 29 Jan 2010; published 23 Feb 2010

Table 2 details the broadband layers selectively lifted off under the excitation waveguides and the liquid-core regions. These layers are designed to be anti-resonant and low loss over a broadband (λ=450 nm to 1100 nm) range. Table 3 details the cross-sectional profile of the liquid-core portion of the device and provides the thickness of the liquid core waveguide.

Table 1. ARROW filter layers design

Layer	Si	SiO_2	SiN	SiO_2	SiN	SiO_2
n	-	1.475	2.05	1.475	2.05	1.475
t_i [nm]	-	840	110	840	439	840

Table 2. ARROW broadband layers design

Layer	Ta_2O_5	SiO_2	Ta_2O_5	SiO_2	Ta_2O_5
n	2.245	1.435	2.245	1.435	2.245
t_i [nm]	90	310	90	310	90

Table 3. Integrated liquid-core ARROW layers design

Layer	Filter Layers	Broadband Layers	Liquid Core	SiN	SiO_2
n	see Table 1	see Table 2	1.33	2.05	1.465
t_i [nm]	-	-	5000	110	5000

2. Integrated filter ARROW fabrication

Creation of selectively defined regions of thin films in planar fabrication can be accomplished by etching or lift-off techniques. For our application, etching procedures are not preferred because ARROW filters have limited thickness tolerances for the dielectric layers. Timing a dry etch procedure to meet these tolerances is challenging. A stop etch layer, placed below the broadband layers to be removed, would complicate the fabrication process and removal of the stop etch from underneath existing broadband layers could prove problematic. Etching processes also introduce surface roughness that would create unacceptably lossy waveguides.

A standard lift-off technique was also found inadequate. In standard lift-off procedures, a directional deposition over a single photoresist or other sacrificial material produces a break in the films. Because plasma-enhanced chemical vapor deposition (PECVD) and sputtering processes are fairly isotropic depositions, a simple rectangular step profile for the sacrificial material cannot be reliably lifted off.

The combination of SU-8 and Polymethylglutarimide (PMGI) resists, as outlined schematically in Fig. 2, provided a reproducible undercut profile that was used successfully to lift off PECVD films. In the case of our notch filters, layers designed to transmit the excitation light are first deposited over the entire silicon substrate (Fig. 2a). A layer of deep UV photo-definable polymer with reproducible undercut and stability at the high temperatures necessary for dielectric thin-film deposition (LOR 30A/PMGI, Microchem) was deposited and patterned with an SU-8 “cap-on” mask (Fig. 2b). The cap-on mask blocks DUV radiation from penetrating and exposing the underlying PMGI and is selective to the developer (AZ300 MIF) used in PMGI processing, producing an undercut layer compatible with lift-off processing (Fig. 2c). Dielectric thin films designed to be anti-resonant and low-loss over a broadband spectrum are deposited over the polymer structure (Fig. 2d). The substrate is placed in Microposit Remover (1165, Shipley) which dissolves the PMGI film cleanly and reveals regions of the filtering films previously deposited (Fig. 2e). A thick top layer of SiO_2 is then deposited over the structure and a solid-core rib waveguide is defined using an ICP RIE process (Fig. 2f).

#121398 - $15.00 USD Received 14 Dec 2009; revised 25 Jan 2010; accepted 29 Jan 2010; published 23 Feb 2010

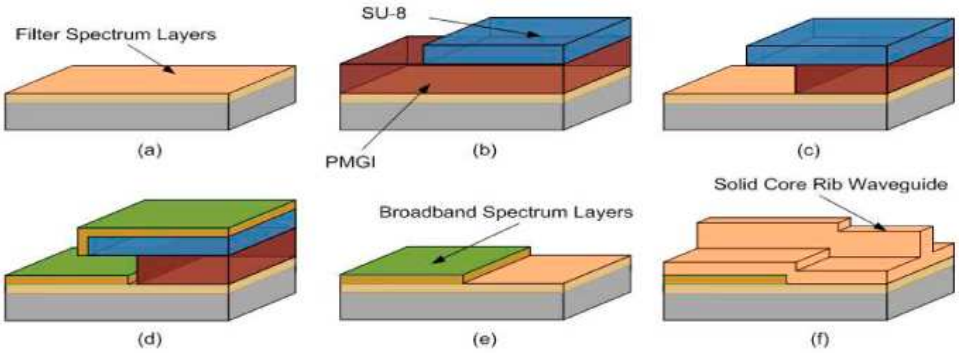

Fig. 2. Integrated filter fabrication by lift-off, a) deposition of filter films, b) patterning of SU-8, c) development of PMGI, d) deposition of broadband films, e) lift-off process, f) patterning of solid-core rib waveguide.

While our technique can work for a wide range of materials and film thicknesses, it was discovered that the lift-off profile provided by SU-8 and PMGI can still be inadequate, if the deposition was too isotropic. As an example, a highly isotropic PECVD recipe was deposited over the lift-off SU-8 and PMGI structure and scanning electron micrographs (SEM) were taken. In Fig. 3a, the dielectric layers have coated the underside of the SU-8 layer and the vertical face of the PMGI. In Fig. 3b, the PMGI was dissolved and removed and a "wall" of thin dielectric layers remained from the coating on the face of the PMGI. When the PECVD process was changed to produce a more directional deposition, a clean break in lift-off films can be produced similar to what is seen in Fig. 3c.

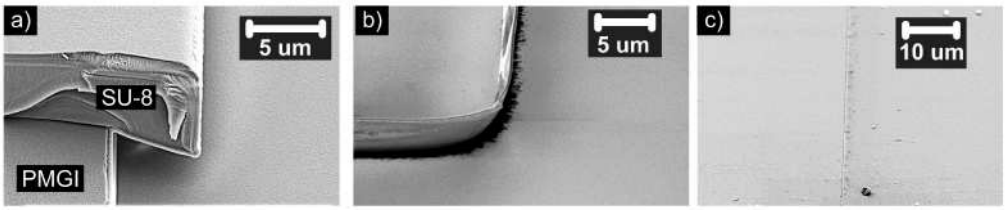

Fig. 3. Isotropic deposition over lift-off polymers, a) coating underside of lift-off polymers, b) vertical "wall" of thin films remaining after the PMGI has been lifted off, c) directional deposition lift-off profile.

3. Optical characterization

To characterize the selectively deposited filters, a white-light setup was used as diagrammed in Fig. 4. Laser pulses (120fs, 75 MHz) at 850nm (Coherent MIRA) were coupled via an optical isolator and an objective lens (O1) into a nonlinear photonic crystal fiber (PCF 790nm zero dispersion wavelength, 1m long). As the high intensity laser pulse propagates through the PCF near the zero dispersion wavelength, a combination of various effects including self-phase modulation, cross-phase modulation, Raman scattering, etc. disperse the pulse into a broad continuum of wavelengths in the visible and near-IR ranges [13]. The white light is then coupled into a single mode fiber (SMF) and directed into the ARROW to be analyzed. The transmitted light is collected by an objective (O2) and sampled in an optical spectrum analyzer (OSA) to determine the spectral response or imaged onto a charge coupled device (CCD) camera to monitor the mode profile.

#121398 - $15.00 USD Received 14 Dec 2009; revised 25 Jan 2010; accepted 29 Jan 2010; published 23 Feb 2010

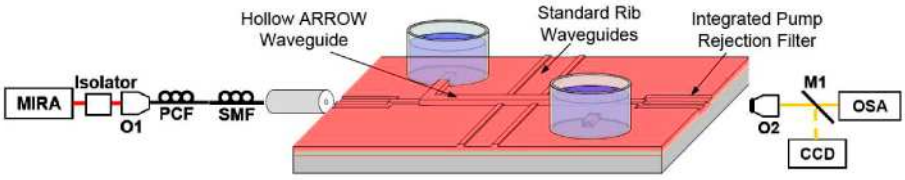

Fig. 4. Optical test setup for white light spectrum analysis

For initial testing of our filter designs, ARROW chips consisting of only solid-core (SiO_2) rib waveguides were created. Core dimensions were 12 µm wide and 4 µm high with a rib etch depth of 2 µm. Each wafer had a collection of waveguides clad with broadband plus filtering ARROW layers (Fig. 5a) and waveguides clad in only filtering ARROW layers (Fig. 5b). Loss coefficients for the long waveguides of both types were found using standard cutback measurement procedures and the results are shown in Fig. 5a,b. Transmission over an 18 mm long section of solid-core filter ARROW showed a rejection of 22 dB with 1.4 nm linewidth. The broadband section loss coefficient was calculated to be α_B ~0.85 cm^1 and the filter section loss at the notch center wavelength was α_F(612.7nm) ~2.6 cm^1. The slight blue shift compared to the design wavelength of 632.8nm was caused by an undergrowth in the resonant layer film thickness. This undergrowth was identified in the preliminary test structures and corrected in later devices.

In addition, waveguides including transitions from broadband to filter sections were used to measure the coupling efficiency between the two profiles, noted by κ_T in Fig. 5c. While an abrupt transition from broadband to filter sections is diagrammed, measurements using SEM show the broadband layers taper in thickness from full designed thicknesses down to no thickness over a length of ~40 µm. κ_T was experimentally deduced from power throughput measurements after taking into account the loss in the broadband and filter sections. The measured κ_T=58% is in excellent agreement with the simulated κ_T=58.4% (FIMMWAVE, ©Photon Design) over a gradual 40 µm long transition between these two waveguide sections.

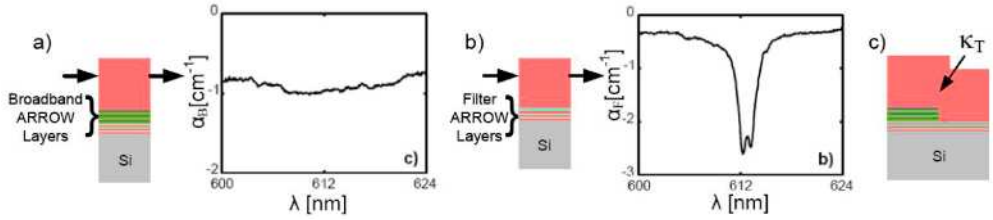

Fig. 5. Optical test of solid-core filtering, a) broadband layer structure and loss coefficient, b) filter region layer structure and loss coefficient, c) lift-off transition from broadband to filter solid-core waveguides.

Complete ARROW platforms including liquid-core waveguide regions (Fig. 1) were then fabricated using the lift-off method described in section 2. The thin-film cross-sections and spectral response are diagrammed in Fig. 6(a), (b). The liquid-core waveguide length (L_{lc}) was lithographically defined to be 4 mm in length. The solid-core filtering waveguides (L_{sc}) can vary in length depending on the level of rejection desired and are generally 2-5 mm long. Within the filtering section, the solid-core rib waveguide dimensions are 12 µm wide by ~5 µm high. Various waveguide coupling efficiencies are defined and diagrammed. Transmission across the chip (~1cm on a side) was measured using the test setup shown in Fig. 4. The transition coupling between solid-core broadband waveguide and solid-core filtering waveguide sections (κ_T) and interface coupling between liquid core waveguide and solid-core waveguide sections (κ_i) reduce overall transmission of the white light.

Figure 6(b) shows the simulated and experimentally measured white light transmissions across a water-filled ARROW with integrated filters. The spectrum shows a fabricated

#121398 - $15.00 USD Received 14 Dec 2009; revised 25 Jan 2010; accepted 29 Jan 2010; published 23 Feb 2010

ARROW designed to reject a HeNe excitation signal (632.8nm) from a Raman or fluorescence experiment. We report a rejection of ~20 dB with linewidth as low as 20 nm over ~9 mm of integrated solid-core filtering ARROW. The simulated spectrum was calculated using typical coupling efficiencies and a 2x2 matrix formulation to determine the loss in each waveguide section [14]. These coupling losses, combined with calculated liquid and solid-core waveguide losses, provide a nominal loss of ~19 dB across the chip in the wavelength range of interest. Linewidth broadening in the measured spectrum is attributed to inhomogeneities in the layer thickness and index across the chip. By improving uniformity of deposition, the linewidth could be narrowed, further improving the filter response. Figure 6c shows an SEM micrograph of the completed liquid-core cross section showing the various dielectric layers that make up the ARROW.

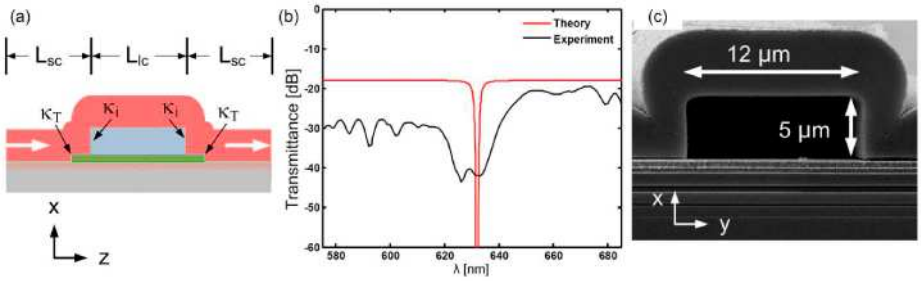

Fig. 6. Optical test of ARROW chip a) side view of liquid-core platform showing broadband sections (L_{lc}) and selectively defined filter regions in solid-core collection waveguides (L_{sc}). Waveguide coupling locations from broadband to filter (κ_T) and liquid-core ARROW to solid-core ARROWs (κ_i) b) simulated (red) and resulting (black) spectrum transmission across entire chip c) SEM of cross sectional profile of liquid-core waveguide.

In integrated optics, the length of filtering waveguides is a large consideration in platform design and implementation. At ~2 dB/mm rejection, our waveguides are comparable to recent inexpensive integrated filters obtaining ~1 dB/mm rejection using long period grating technologies [15,16] but the ARROW has a larger free spectral range. Overall transmission from chip edge to chip edge is limited by various efficiencies described previously [17]. However, in an application focused on fluorescence or Raman signal collection, the signal would only have to pass through half the liquid core waveguide and a single solid-core filtering waveguide to the photo detector.

4. Conclusion and summary

In summary, we have presented a method for integrating optical filters into standard ARROW processing. The lift-off method explored is compatible with aspects of planar fabrication such as high temperature and non-directional film deposition. We fabricated and tested the lift-off method for filter integration and found comparable results to other integrated filtering technologies.

By integrating filters, we can improve the ARROW platform in a number of ways. With a lift-off method, we free ourselves from various planar fabrication constraints. This offers design flexibility to produce different spectral characteristics at various locations on a single chip. This flexibility can be useful in creating platforms suited for experiments involving multiple excitation and signal wavelengths, e.g. fluorescence resonance energy transfer. Also, a chip with integrated filters would allow photo detectors and other external components to eventually move onto the chip as well, creating a more compact and self-contained platform.

Acknowledgments

This work was supported by the NIH/NIBIB (R01EB006097), NSF (ECS-0528730, ECS-0528714), the W.M. Keck Center for Nanoscale Optofluidics at the University of California at Santa Cruz. B.S.P. acknowledges support from the SMART Scholarship for Service Program.

#121398 - $15.00 USD Received 14 Dec 2009; revised 25 Jan 2010; accepted 29 Jan 2010; published 23 Feb 2010